



**HAL**  
open science

## Characterization and 3D printability of poly (lactic acid)/acetylated tannin

Jingjing Liao, Nicolas Brosse, Antonio Pizzi, Sandrine Hoppe, Xiaojian Zhou,  
Guanben Du

► **To cite this version:**

Jingjing Liao, Nicolas Brosse, Antonio Pizzi, Sandrine Hoppe, Xiaojian Zhou, et al.. Characterization and 3D printability of poly (lactic acid)/acetylated tannin. *Industrial Crops and Products*, 2020, 149, pp.112320. 10.1016/j.indcrop.2020.112320 . hal-02508080

**HAL Id: hal-02508080**

**<https://hal.univ-lorraine.fr/hal-02508080v1>**

Submitted on 13 Mar 2020

**HAL** is a multi-disciplinary open access archive for the deposit and dissemination of scientific research documents, whether they are published or not. The documents may come from teaching and research institutions in France or abroad, or from public or private research centers.

L'archive ouverte pluridisciplinaire **HAL**, est destinée au dépôt et à la diffusion de documents scientifiques de niveau recherche, publiés ou non, émanant des établissements d'enseignement et de recherche français ou étrangers, des laboratoires publics ou privés.

# 1 Characterization and 3D printability of poly (lactic acid)/acetylated tannin 2 composites

3 Jingjing LIAO<sup>a,b,c</sup>, Nicolas BROSSE<sup>b\*</sup>, Antonio PIZZI<sup>b</sup>, Sandrine HOPPE<sup>c</sup>, Xiaojian ZHOU<sup>a\*</sup>, and Guanben  
4 DU<sup>a</sup>

5 <sup>a</sup> Key Laboratory for Forest Resources Conservation and Utilisation in the Southwest Mountains of China  
6 (Southwest Forestry University), Ministry of Education, Kunming, 650224, PR China

7 <sup>b</sup> LERMAB, University of Lorraine, Boulevard des Aiguillettes BP 70239, 54506 Vandœuvre-lès-Nancy, France

8 <sup>c</sup> LRGP, University of Lorraine, 1, Rue Grandville, BP 451, 54001 Nancy Cedex, France

9 \* Correspondence: [nicolas.brosse@univ-lorraine.fr](mailto:nicolas.brosse@univ-lorraine.fr); xiaojianzhou@hotmail.com

10  
11 **Abstract:** In this study, a three-dimensional (3D) printing filament prepared from  
12 poly (lactic acid) (PLA) and acetylated tannin via a twin-screw extruder was reported.  
13 The impact of acetylated tannin loading content on the final properties of the  
14 resulting composite materials and their 3D printability were investigated. The  
15 experimental results indicate that PLA can be compounded with up to 20 wt%  
16 acetylated tannin without any obvious deterioration in the tensile property. The  
17 resulting composites acquired better degradation rate in aquatic system compared  
18 with neat PLA, especially in alkaline medium. Moreover, all composites are printable  
19 and showed generally good printing quality with brown color, however, this is  
20 limited to temperatures reasonably below 220°C to avoid printing defects, especially  
21 at high loadings of acetylated tannin.

22  
23 **Keywords:** poly (lactic acid), acetylated tannin, composite, degradation, 3D  
24 printability

## 25 26 1. Introduction

27 Additive manufacturing, commonly known as three-dimensional (3D) printing, is a  
28 promising manufacturing technology whose related numerous applications have been  
29 explored in the fields like construction, manufacturing, healthcare and medicine, art and  
30 fashion, food industry (Lee et al., 2017; Liu et al., 2019). With this technique, customized  
31 complex and high-resolution three-dimensional parts can be rapidly built through

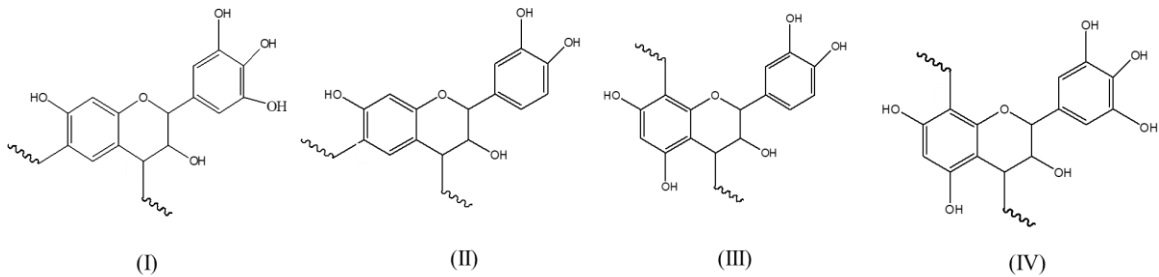
32 successive layer-by-layer deposition of materials like plastic, metal, ceramics, or living  
33 cells (Tappa and Jammalamadaka, 2018). For producing thermoplastics prototype parts,  
34 fused deposition modeling (FDM) or melt-extrusion 3D printing is the most widely used  
35 additive manufacturing technique.

36 Poly(lactic acid) (PLA) is one of the most popular 3D printing thermoplastic materials  
37 due to its printability, favorable mechanical properties, and biocompatibility. It is an  
38 renewable and biodegradable polyester that can be synthesized directly through  
39 polycondensation of lactic acids or ring-opening polymerization of lactides (Ren, 2011).  
40 PLA can be also incorporated with sustainable materials or biopolymers (e.g. wood  
41 powder, plant fiber, cellulose, lignin, hemicellulose) for the purpose of reinforcing  
42 and/or specific functions, and/or reducing cost. However, studies of these PLA-based  
43 bio-composites as 3D printing materials are still limited (Bajpai et al., 2014; Basu et al.,  
44 2017; Murariu and Dubois, 2016). Sustainable materials or biopolymers applied as 3D  
45 printing feedstock are promising substitutes for fossil-based fillers due to their  
46 sustainability, biodegradability, and cost-efficient characteristics. For instance, the  
47 presence of wood powder in 3D printing, PLA filaments displays higher stiffness and less  
48 abrasive properties compared to other composite filaments, such as carbon-fiber filled  
49 PLA filaments and metal-filled PLA filaments (Guo et al., 2018). Fibers derived from  
50 wood, bamboo, and cellulose were also investigated as feedstock for PLA-based  
51 filaments because of their positive effects on the mechanical properties and heat  
52 resistance of PLA matrix (LI et al., 2016; Long et al., 2019). Hemicellulose has been  
53 investigated to partially replace PLA as feedstock material in 3D printing (Xu et al.,  
54 2018). This combination makes use of the characteristics of hemicelluloses such as  
55 biocompatibility, biodegradability, and presence of versatile active sites for biomedical  
56 applications. PLA combined with lignin has attracting characteristics such as antioxidant,  
57 antifungal and antimicrobial capacities, resistance to UV-radiation, and fire-retardant  
58 properties (Kai et al., 2016). One example was reported to study PLA/lignin composites  
59 for 3D printing (Gkartzou et al., 2017). However, the lignin aggregation and its low  
60 compatibility with PLA matrix caused imperfect printed objects and surface roughness,

61 even at low loading content (5 wt%). According to the published literature as yet, it  
62 appears that the dispersion and distribution of fillers are key factors for processing 3D  
63 printing materials (Nguyen et al., 2018).

64 Condensed tannins are interesting abundant and sustainable biopolymers for 3D  
65 printing, however, there is no related research work about their applications in the field  
66 of 3D printing to date. Condensed tannins are mainly composed of flavonoid units in  
67 varying degrees of condensation (**Erreur ! Source du renvoi introuvable.**) and they can  
68 be easily extracted from soft tissues of woody plants like leaves, needles, and bark using  
69 water or organic solvent (Pizzi, 1980). They display great potential as component of PLA  
70 bio-composites due to some interesting characteristics like antioxidant (Koleckar et al.,  
71 2008), antimicrobial (Ge et al., 2003) and stabilizing properties (Liao et al., 2019; Olejar  
72 et al., 2016; Tomak et al., 2018). Over the past few years, tannins have been  
73 investigated as functional additives or at least a component of polymeric composites.  
74 For instance, tannins have been reported as stabilizing additive with antioxidant and UV-  
75 protective properties on polypropylene (Ambrogi et al., 2011; Samper et al., 2013),  
76 polyethylene (Bridson et al., 2015), poly(vinylchloride) (PVC) (Shnawa et al., 2015), and  
77 polyvinyl alcohol (Zhai et al., 2018). Anwer reported a native tannin as a filling  
78 component of PLA composite material (Anwer et al., 2015), where poor adhesion  
79 between tannin and PLA matrix as well as dispersion of tannin in PLA were found,  
80 thereby, poor tensile strength was noticed even at higher filler content (15%).  
81 Modifications of tannins, like esterification and hydroxypropylation, have been proved  
82 to enhance the compatibility and dispersion capacity to various plastics (D. E. García et  
83 al., 2015; Gaugler et al., 2007; Grigsby et al., 2014, 2015, 2013; Grigsby and Kadla, 2014).  
84 Grigsby and co-workers (Grigsby et al., 2015) modified tannin with ester-bearing long  
85 chain, which lowered the melting temperature and claimed this could significantly  
86 reduce the incompatibility with PLA matrix, leading meanwhile to easier processability.  
87 However, the substitution of higher chain length on tannin flavonoid units becomes  
88 progressively more difficult due to the elevated steric hindrance. In another extended  
89 study, Grigsby carried out a high loading content of esterified tannin (50%) as

90 reinforcing material for PLA fine fiber processed via melt spinning in the presence of  
91 transesterification catalyst (Grigsby and Kadla, 2014). This successful incorporation of  
92 esterified tannin onto PLA indicated the possibility to process esterified tannin filled PLA  
93 filaments for 3D printing. Esterification can reduce the hydrophilicity of tannin, reducing  
94 the clogging at the printing nozzle and discontinuous layer deposition during printing  
95 process due to good dispersion and distribution of tannin onto the polymer matrix.



96

97

Figure 1. Structure of four main flavonoid units of condensed tannins

98 The present study will focus on developing a new approach to utilize condensed  
99 tannin obtained from mimosa wood barks for partial replacement of PLA in 3D printing  
100 parts and investigate the feasibility of melt-extrusion 3D printing. For this purpose,  
101 mimosa tannin was acetylated to decrease its initial hydrophilicity. Such treatment has  
102 been proven to enhance the compatibility of tannin and thermoplastic polymeric  
103 matrixes without severe agglomeration (Gaugler et al., 2007; Grigsby et al., 2013). The  
104 composite was processed in a twin-screw extruder and the impact of the loading level of  
105 acetylated tannin (AT) on the final properties of the resulting composite materials was  
106 evaluated in terms of the tensile property, the changes in crystallization, thermal  
107 degradation, changes in color, and degradation rate in aquatic system. Besides, the  
108 feasibility of melt-extrusion 3D printing of PLA/AT composite was also investigated.

## 109 2. Materials and Methods

### 110 2.1. Materials

111 PLA trademarked under the name Ingeo™ Biopolymer (Grade 3D850) with a melt  
112 flow index of 7-9 g/10min was obtained from Nature works LLC (Minnesota, USA).  
113 Mimosa tannins were purchased from Silva Chimica, Mondovi, Italy. Acetic anhydride

114 used to acetylate tannin and pyridine, a catalyst for tannin acetylation, were supplied  
115 from Sigma-Aldrich and Acros-Organics, respectively. Three buffers purchased from  
116 Sigma-Aldrich were used for degradation tests, including phosphate buffer (pH=4.0),  
117 sodium carbonate buffer (pH=10.0), and phosphate Buffered Saline (PBS, pH=7.4).

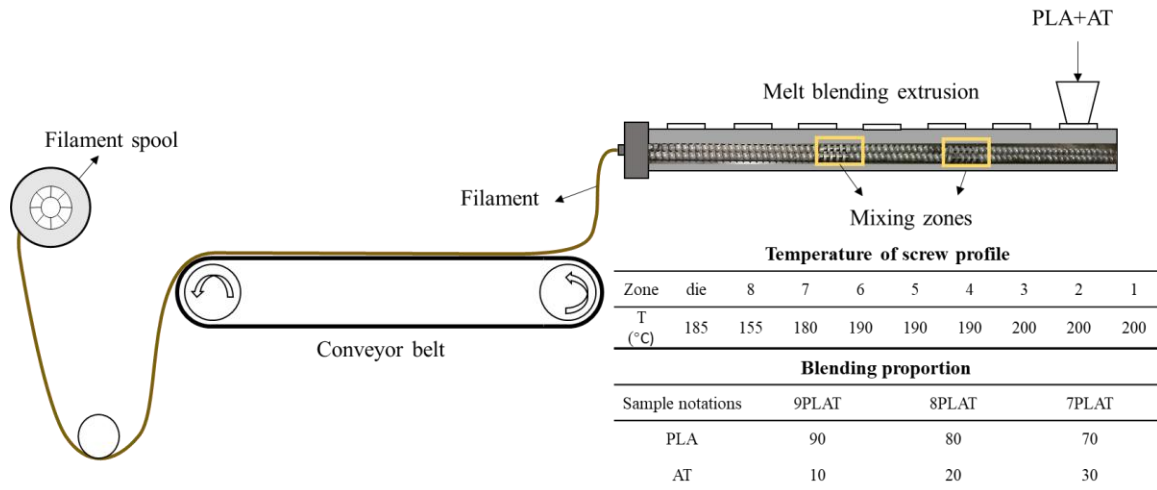
## 118 **2.2. Preparation of PLA/AT Composites**

### 119 2.2.1. Tannin acetylation

120 Acetylation of mimosa tannin was described elsewhere by using acetic anhydride  
121 and pyridine as catalyst (Nicollin et al., 2013). Mimosa tannin was mixed with acetic  
122 anhydride in a weight ratio of 1:5 with 1 wt% pyridine (based on tannin) as catalyst in a  
123 round bottom flask fitted with a condenser. The mixture was heated to 60°C under  
124 stirring for 6 h. After the acetylation is achieved, the suspension was precipitated in iced  
125 water and centrifuged to recover the acetylated tannin powder, which was washed 5  
126 times with distilled water and finally air-dried at room temperature for several days.

### 127 2.2.2. Composite filament preparation

128 PLA was ground into powder by a grinder to ensure simplistic mixing with tannin.  
129 Then, PLA and acetylated tannin (AT) powder were dried in an oven at 80°C for more  
130 than 12 h to remove any absorbed water on the surface. A twin-screw extruder (Thermo  
131 Scientific™ Process 11, Villebon-Sur-Yvette, France) was used to blend PLA powder and  
132 AT. Two mixing zones of screw profile can guarantee high level of homogeneous  
133 dispersion of AT in PLA. The temperature of the heating zones and the die along the  
134 extruder barrel ranged are shown in Figure 2. The filaments were extruded through melt  
135 blending extrusion with a rotation rate of 80 rpm via a nozzle diameter of 4 mm. A  
136 filament with a diameter of  $1.75 \pm 0.1$  mm was obtained by controlling the speed of  
137 spool rotation and conveyer belts then the 3D printable filaments were collected by a  
138 spool.



139

140

141 *Figure 2. Composite filaments preparation via melt blending extrusion: the tables show the*  
 142 *parameters of screw profile and blending components proportions*

143 2.2.3. 3D printing process

144 An open-source 3D printer named Mondrian 3.0 was used to print scaffold (20.1 ×  
 145 20.1 × 3 mm) and standard dog bones (ISO 527, type 1A) using PLA/AT filaments at  
 146 190°C. Abundant of filament was needed to construct dog bone specimen, thus, we  
 147 prepared only one dog bone specimen due to the limited filament amounts. The  
 148 scaffolds were printed using PLA and PLA/AT composite filaments under three printing  
 149 temperature (180°C, 200°C, 220°C). The used printing parameters are shown in Table 1.  
 150 The scaffold and dog bone were designed by using a Slic3r program and printing process  
 151 were controlled by Pronterface software.

152

*Table 1. 3D printing parameters*

Printing temperature	180 - 220°C
Layer height	0.2 mm
Infill density	100%
Infill pattern	linear
Layer angle	45°
Printing speed	12 mm/s

**153 2.3. Characterizations**

154 The acetylation of tannin was confirmed by NICOLET 6700 FT-IR spectrometer in  
155 attenuated total reflection (ATR) mode with a resolution of  $4\text{ cm}^{-1}$  and a total of 16  
156 scans in the range  $400\text{-}4000\text{ cm}^{-1}$ .

157 Instron tensile testing machine (model 5569, Norwood, MA, USA) equipped with a  
158 50 kN load cell was used for tensile strength tests with a cross-head speed  $1\text{ mm/min}$   
159 according to EN ISO 527:1996. The whole testing process was performed at room  
160 temperature and each sample has four repetitions. The tested dog-bone shaped  
161 specimens (ISO 527, type 1A) were previously molded with a micro-injection molder  
162 (Micro 15, DSM Xplore, Sittard, Netherlands).

163 A scanning electron microscopy (SEM, JSM-6490LV, Tokyo, JAPAN) with an  
164 acceleration voltage of  $5\text{ kV}$  was applied to observe the morphology of a 3D printed  
165 scaffold. The scaffolds were sputter-coated with a thin layer of carbon before scanning.

166 A study on the thermal characteristics, in terms of the melting temperature ( $T_m$ ) and  
167 crystallization temperature ( $T_c$ ), was undertaken under a nitrogen flow of  $50\text{ mL/min}$  by  
168 using a METTLER TOLEDO differential scanning calorimeter (DSC). A scanning rate of  
169  $10^\circ\text{C/min}$  within the temperature range of  $30^\circ\text{C}$  to  $220^\circ\text{C}$  and  $220^\circ\text{C}$  to  $-10^\circ\text{C}$  in the  
170 second scanning cycle was carried out. The measurements were conducted using  
171 aluminum crucibles with a total sample weight of  $5.00 \pm 1\text{ mg}$ . The values for melting  
172 temperatures ( $T_m$ ), enthalpies of melting ( $\Delta H_m$ ) and crystallization ( $\Delta H_c$ ) were analyzed  
173 using STARE software.  $\Delta H_m^0$  is the enthalpy of melting for 100% crystallized PLA, which is  
174 equal to  $93.7\text{ J/g}$  (Yamoum et al., 2017), and  $w$  is the weight fraction of PLA. The  
175 crystallization percentage ( $X_c$  %) was estimated using the following equation:

$$X_c (\%) = \frac{\Delta H_m - \Delta H_c}{\Delta H_m^0 \times w} \times 100\% \quad (1)$$

176 The degradation behavior of AT-filled PLA was characterized with the help of a  
177 thermogravimetric analyzer (TGA, METTLER TOLEDO, Columbus, Ohio, USA) under air



178 flow of 50 mL/min from 30 to 600°C. The heating rate was controlled at 10°C/min and  
179 the weight of each sample was 5-10 mg.

180 **Color measurements.** PLA is a colorless and transparent polymer, thus, it generally  
181 colorize with dyes (Hussain et al., 2015; Scheyer and Chiweshe, 2001). Tannin can  
182 colorize PLA filaments due to its brown nature, which is a good feature for 3D printed  
183 parts. The coloration of PLA filaments with acetylated tannin was investigated by a  
184 spectrophotometer (X-rite, model 5P60, Regensdorf, Switzerland) based on the  
185 international commission on illumination (CIE) system. Three parameters L\*, a\* and b\*  
186 were used to evaluate the colors of filaments, respectively. L\* represents the scale of  
187 lightness, the value of 0-100 refers to perfect black to white. The value of a\* and b\*  
188 stands for the color of the red-green and the yellow-blue character, respectively, in  
189 which positive values represent redness or yellowness while negative values indicate  
190 greenness and blueness (Lai So et al., 2014).

191 **Water absorption.** The hydrophobicity of the filaments was characterized by  
192 measuring their level of water absorption (Figueira et al., 2017). Each filament was cut  
193 into a length of  $70 \pm 1$  mm and submerged into 50 mL of distilled water in a plastic tube  
194 for 30 days at room temperature. Before submerging the tested filaments into the  
195 water, the filaments were vacuum-dried for 6 h at 80°C and then measured the dried  
196 weight ( $W_0$ ). After 30 days, the specimens were taken out from water and wiped using  
197 filter paper. Then the weight was recorded as  $W_1$ . The water uptake of PLA filaments  
198 and AT-filled filaments was calculated according to the following equation:

$$\text{Water absorption (\%)} = \frac{|W_1 - W_0|}{W_0} \times 100 \quad (2)$$

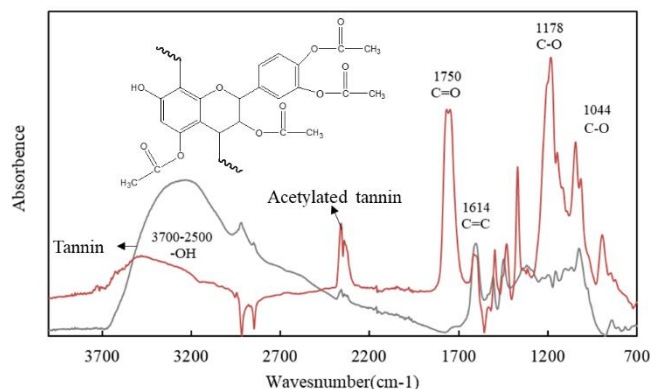
199 **Immersion in solvent.** In order to understand the degradation of PLA/AT composites  
200 in aquatic system, printed specimens of dimensions  $2.5 \times 30 \times 2$  mm were immersed in  
201 buffer solutions (pH=4, pH=10) and PBS solution (pH 7.4) at 40°C for 50 days in an oven.  
202 The initial weight ( $W_0$ ) of each specimen was recorded before soaking into the solvent in  
203 glass tube containing 50 mL buffer solution. After 50 days, the samples were removed  
204 from the tubes and washed 3 times with distilled water prior to final dry in oven at 40 °C

205 for 12 h. The weight of each specimen was denoted as  $W_1$ . The weight loss was  
206 calculated based on the equation (2).

### 207 3. Results and discussion

#### 208 3.1. Characterization of acetylated tannin

209 The hydrophilic characteristic of tannin render it incompatible with hydrophobic or  
210 semi-hydrophobic polymers. This necessitates the modification of tannin for solving this  
211 problem. Tannin acetylation was suggested to develop reasonable miscibility with PLA  
212 (Grigsby and Kadla, 2014). Figure 3 presents the FTIR spectra of tannin and tannin after  
213 being acetylated. The spectrum of tannin reveals a broad band centered at  $3250\text{ cm}^{-1}$   
214 and can be ascribed to -OH stretching vibrations while the peak at  $1614\text{ cm}^{-1}$  refers to  
215 aromatic ring stretching vibration. This latter signal corresponding to a function  
216 unaffected by the acetylation reaction which can be considered as an invariant band.  
217 Compared to the band at  $1614\text{ cm}^{-1}$ , the sharp decrease of the -OH and emergence of a  
218 new strong one at  $1750\text{ cm}^{-1}$ , which is typical of C=O stretching, representing ester  
219 functional group, proves that the acetylation process was undertaken effectively (Luo et  
220 al., 2010). Besides, the increased absorption at  $1178\text{ cm}^{-1}$  and  $1044\text{ cm}^{-1}$ , ascribed to C-O  
221 stretching, is also in accordance with the structure of acetylated tannin (Smith, 2018;  
222 Vila et al., 2016).



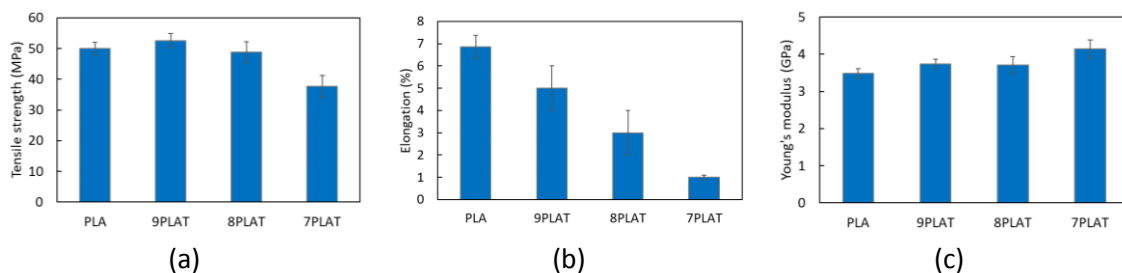
223

224

Figure 3. FTIR spectra of tannin and acetylated tannin

#### 225 3.2. Mechanical properties of PLA/AT composites

226 The mechanical properties of PLA and PLA/AT composites are given in Figure 4.  
227 Tensile strength of composite materials generally relies on the stress transfer capacity  
228 between fillers and polymer matrix, which is significantly affected by the interfacial  
229 adhesion of particle and matrix, particle size, as well as particle distribution (Fu et al.,  
230 2008). The dispersion of AT into a thermoplastic polymer without severe agglomeration  
231 has been previously achieved by enhancement of the hydrophobic character of tannin  
232 (Gaugler et al., 2007; Grigsby et al., 2013). Therefore, unlike native tannin-filled PLA  
233 (Anwer et al., 2015), PLA incorporated with 10% and 20% AT did not exhibit significant  
234 effects on tensile strength of the resulting composites (Figure 4, a). While PLA  
235 incorporated with 30% AT encountered a decrease of tensile strength because higher  
236 biopolymer content generally caused filler agglomeration during melt blending process  
237 could result in poor particle distribution. Besides, higher loading of AT increases its  
238 interfacial area with PLA, which worsens the situation especially in absence of interfacial  
239 adhesion due to lack of virtual chemical bonds between AT and PLA. A lower elongation  
240 at break was noticed for PLA/AT composites compared with the neat PLA (Figure 4, b),  
241 which again highlights the fact that the acetyl part as a modifying agent for tannin does  
242 not possess any plasticizing effect to balance the developed interfacial adhesion as a  
243 result of acetylation, which causes premature failure. In Figure 4 (c), Young's moduli  
244 increased as a function of AT loading since the filling component restricts the molecular  
245 mobility of the polymeric chain yielding a better static adhesion (Wacker et al., 1998). A  
246 similar result was previously noted for lignin-filled PLA system (Spiridon et al., 2015; Vila  
247 et al., 2016).



248 *Figure 4. Tensile parameters of PLA/AT composites: tensile strength (a), elongation (b) and*  
249 *Young's modulus (c)*

### 250 **3.3. Differential scanning calorimeter**

251 DSC was performed in order to detect the glass transition, crystallization and melting  
252 temperatures of PLA and PLA/AT composites. DSC thermograms of PLA and PLA  
253 incorporated with various contents of AT are shown in Figure 5 and the results from the  
254 second heating and first cooling cycles are collected in Table 2. The incorporation of AT  
255 showed no significant effect on the melting ( $T_m$ ) and the glass transition ( $T_g$ )  
256 temperatures, are consistent with prior studies (Anwer et al., 2015; Grigsby et al., 2014;  
257 Grigsby and Kadla, 2014). This means AT has little influence on intermolecular  
258 interactions or chain flexibility of PLA polymer chains (Müller et al., 2014). While the  
259 enhancement of  $T_c$  refers to the composite filaments are more difficult to undergo cold  
260 crystallization in comparison with pure PLA filaments and so require higher  
261 temperatures (Dong et al., 2017). As can be found in Table 2, the crystallinity of PLA/AT  
262 composites` is gradually decreasing with a corresponding decrease in the enthalpy of  
263 crystallization as a function of AT content. Therefore, the PLA/AT composites became  
264 too amorphous to be more liable to undergo higher degradation rates. This feature  
265 most likely benefits to the short-term application like implantable devices in biomedical  
266 applications (Lyu and Untereker, 2009) since the degradation of PLA occurs during a  
267 generally long period (Karamanlioglu et al., 2017; Tokiwa and Calabia, 2006).

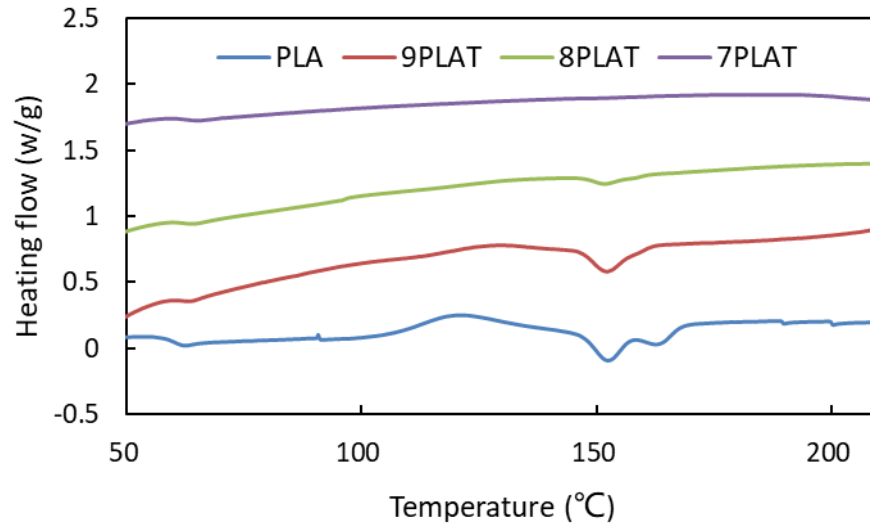


Figure 5. DSC thermograms of PLA and PLA/AT composites

Table 2. DSC results of PLA and PLA/AT composites

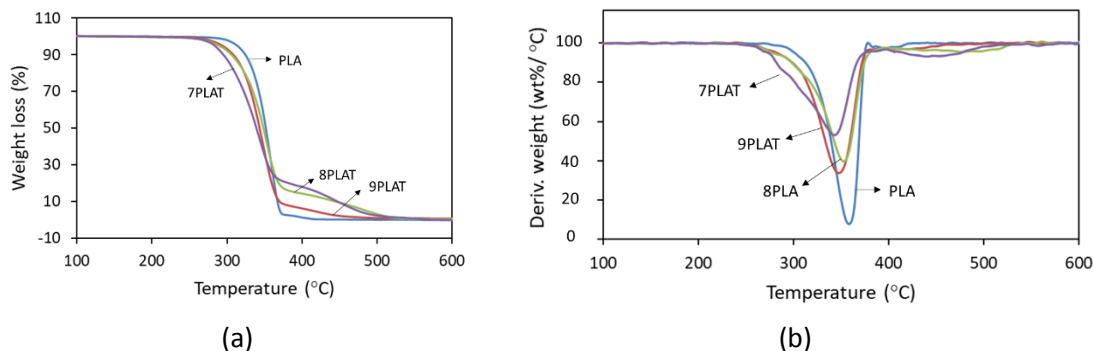
Sample	$T_g$ (°C)	$\Delta H_c$ (J/g)	$T_c$ (°C)	$\Delta H_m$ (J/g)	$T_m$ (°C)	$X_c$ (%)
PLA	56.7	14.2	120.2	20.4	152.5	6.6
9PLAT	56.3	4.23	127.5	10.9	152.6	7.9
8PLAT	56.8	0.78	129.4	3.01	151.9	3.0
7PLAT	58.6	0.26	129.7	0.06	151.1	--

Note: "--" means that no crystallization percentage.

### 3.4. Thermogravimetric analysis

The thermal behavior of PLA and PLA/AT composites was studied via thermogravimetric analysis under air atmosphere. The weight loss and DTG data are plotted in Figure 6 as a function of temperature. Each sample sharply degraded in a one-step process started at 250°C and continued to 370°C, which is also corroborated from the single peak in the DTG profile. The results demonstrated additionally that the incorporation of AT into to PLA matrix resulted in a decrease of the thermal stability, presumably due to the drop in crystallinity (see Table 2). This observation is generally found in PLA biocomposites (Boruvka et al., 2019; Grigsby et al., 2014; Zhang et al.,

282 2017). The onset of degradation for all PLA/AT composites was very close to pristine  
283 PLA (250°C) while the major decomposition took place at 350°C. Consequently, a  
284 printing temperature below 250°C is considered suitable for PLA/AT composites and no  
285 decomposition should be undertaken under these conditions.



286 *Figure 6. Thermal gravimetric traces of PLA and PLA/AT composites (a) and their relevant DTG*  
287 *curves (b).*

### 288 3.5. Water absorption and degradation in solvent

289 PLA is a well-known degradable polymer, however, the total degradation of PLA into  
290 carbon dioxide, water, and methane in the environment generally lasts from several  
291 months to two years (Karamanlioglu et al., 2017). Moisture easily results in the  
292 hydrolyzation of PLA, therefore, water absorption capacity has been considered as an  
293 important factor to the degradability of PLA (Yew et al., 2005) when exposed to humid  
294 atmosphere. Degradation behavior of material in different pH condition is an important  
295 characteristic for many applications.

296 As presented in Figure 7 (a), PLA/AT composites exhibited a higher water absorption  
297 compared with the neat PLA, which may result from the decrease of crystallinity. The  
298 water absorption is related to its rate of diffusion into the composites and responsible  
299 for faster degradation of PLA/AT composites in various aqueous solutions (Figure 7, b).  
300 This characteristic is positive for medical applications because the PLA-based implants  
301 are firstly hydrolyzed in vivo by body fluids after absorbing water, which causes the  
302 breaking of the ester bonds (Yew et al., 2005). In this study, the phosphate-buffered  
303 saline (PBS) solution (pH=7.4) was used to represent the body fluids in neutral

304 conditions, while phosphate buffer (pH=4.0) and sodium carbonate buffer (pH=10) are  
 305 applied to investigate the degradation of composite material in acidic and basic  
 306 conditions. All tested samples in aqueous environments exhibited higher degradation  
 307 rate with increasing the AT content. The faster degradation that appeared in strongly  
 308 basic condition is the easier random ester cleavage, whereas, under acidic conditions, it  
 309 proceeds via chain-end cleavage, which is more time-consuming (Elsawy et al., 2017).

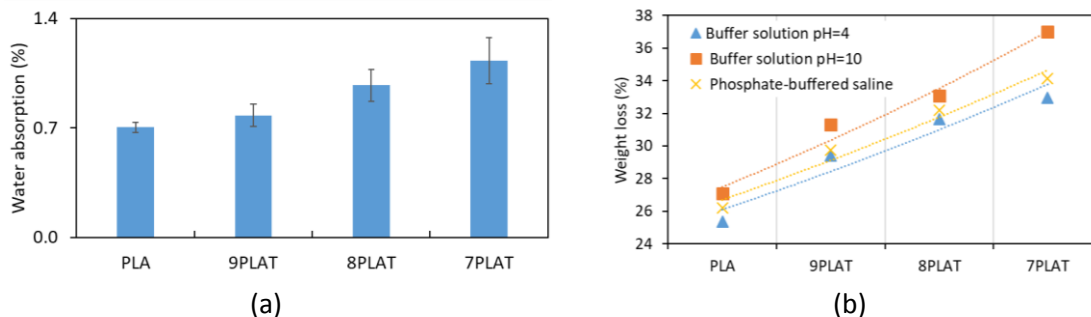


Figure 7. Water absorption of PLA with various AT contents over 30 days(a) and degradation in different solvent media over 50 days (b).

### 310 3.6. PLA/AT composites for 3D printing application

311 Color is an important appearance factor for 3D printing products. As can be seen  
 312 from Table 3, PLA is a colorless transmitting polymer. The combination of PLA with dyes  
 313 for producing vibrant colors is necessary for commercial applications (Scheyer and  
 314 Chiweshe, 2001). From the optical image of the filaments (Table 3), PLA/AT composites  
 315 displayed brown colors and lost transmitting characteristic. These composites had lower  
 316 L\* value which translates into a decrease of lightness. When PLA was compounded with  
 317 more AT, an increasing trend was observed from the increasing a\* and b\* values,  
 318 exhibiting more green hue and blue hue, respectively. Therefore, PLA/AT composites  
 319 could be promising colored filaments for 3D printing products.

Table 3. Color measurements of PLA and PLA/AT composite

sample	Image of PLA and PLA/AT composites	L*	a*	b*
--------	------------------------------------	----	----	----

PLA		70.93	+0.91	+5.43
9PLAT		28.07	+7.91	+7.80
8PLAT		29.77	+9.09	+10.05
7PLAT		31.42	+10.22	+8.41


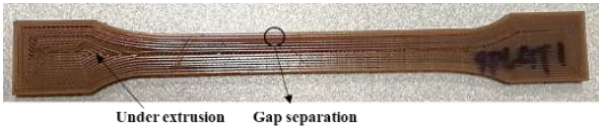

321 The model of dog bone specimens for tensile testing was used to evaluate the  
322 printability of PLA/AT composites, the printed specimens and their tensile strength  
323 results are collected in Table 4. The digital images of printed PLA/AT composites



324 revealed that the specimens exhibited some defects during printing, either under-  
 325 extrusions or in fill and outline separations. These printed issues are not only due to the  
 326 setting of the printing parameter but also may be caused by the imperfect dispersion  
 327 and agglomeration of the filler (Filgueira et al., 2017). Imperfect printing is commonly  
 328 found in composite materials given that the presence of fillers in polymeric matrixes  
 329 change their characteristics and consequently affect their printability (Nguyen et al.,  
 330 2018). Therefore, a correlation between the features of printing process with the AT-  
 331 filled composite filaments is a key factor to obtain qualified printed objects. This issue  
 332 will be considered more intensively in our future work.

333 The materials derived from the melt-extrusion 3D printing process commonly  
 334 showed a lower tensile strength compared to comparable specimens obtained by  
 335 traditional manufacturing methods (Cruz Sanchez et al., 2017). The relatively higher  
 336 porosity of the dog bones caused during 3D printing may probably justify this finding  
 337 (Filgueira et al., 2017). Another possible reason could be related to the poor interlayer  
 338 adhesion of the printed specimens because the mechanical properties of printed part  
 339 depends on the interlayer adhesion (Bakrani Balani et al., 2019). As a whole, the  
 340 strength of printed specimen was very close to that processed by traditional  
 341 manufacturing methods (Figure 4).

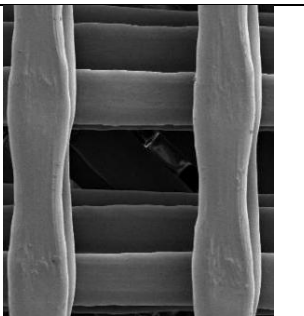
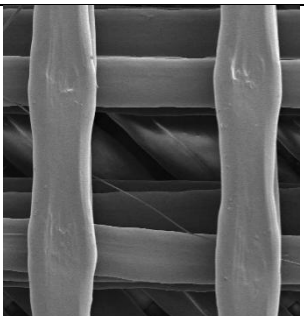
342 *Table 4. Printed dog bone specimens and their tensile parameters*

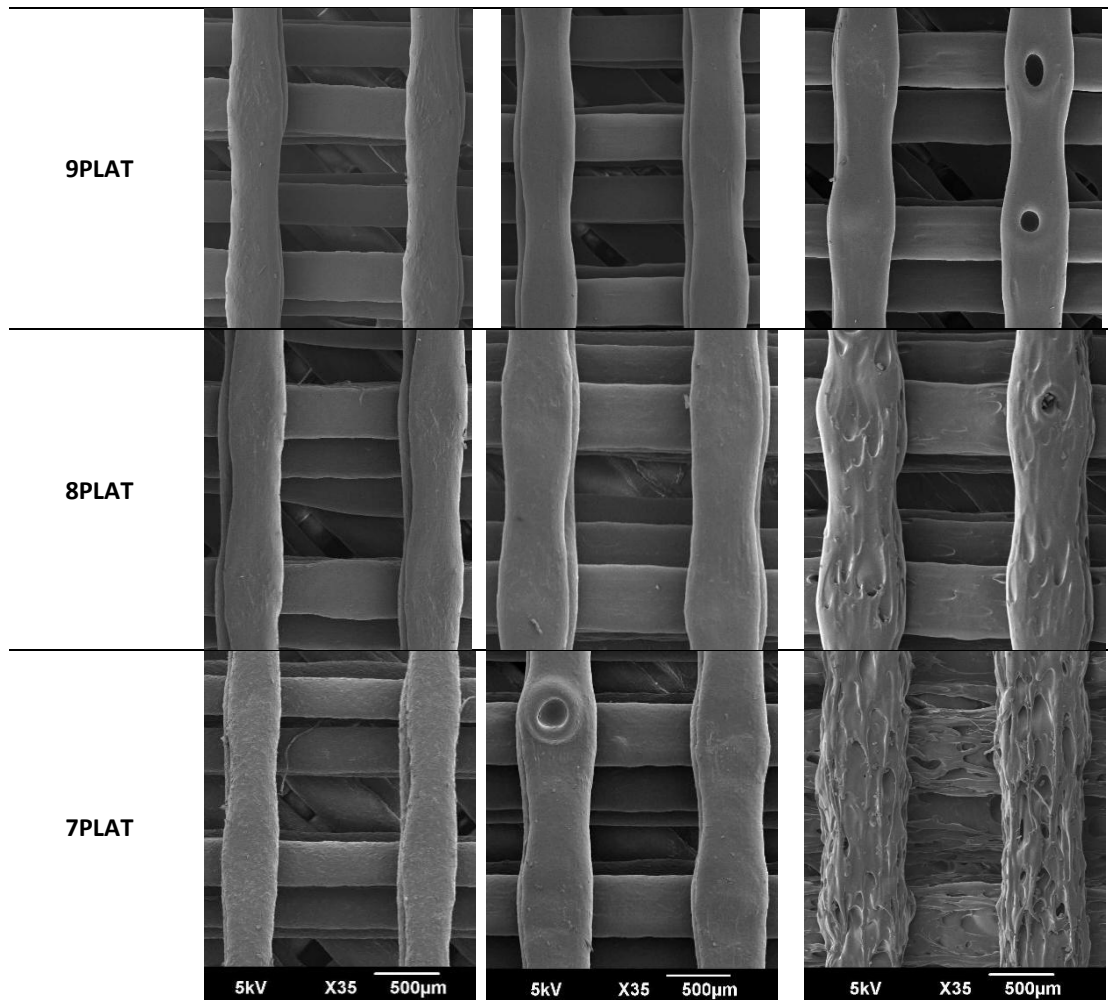
specimen	Image	Young's modulus GPa	Tensile strength MPa
PLA		2.6	27
9PLAT		2.1	26
7PLAT		2.9	31

343 For a specific material, the temperature is one of the most important parameters to  
 344 control the shear viscosity and flow rate for offering successive layer deposition. The  
 345 dimensional stability of each printed layer depends on the rapid solidification capacity  
 346 via improved heat dissipation (Nguyen et al., 2018). Thus, the temperature should be  
 347 carefully selected for validating the balance between flowability and solidification. For  
 348 this purpose, the effects of temperature on the printability of PLA/AT composites and  
 349 morphology of printed specimens were investigated by printing a scaffold prototype.

350 SEM images of the printed scaffolds at different temperatures are displayed in Table  
 351 5. Filaments made from PLA/AT composites are printable at a temperature range from  
 352 180 to 220°C. However, the surface morphology was mostly affected especially at higher  
 353 temperatures. It is worth to notice that both lower and higher printing temperatures  
 354 result in unsatisfying faults on the surface, namely, high roughness and phase  
 355 separation, respectively, when PLA incorporated with a higher AT content (e.g. 7PLAT).  
 356 This highlights a strong correlation between high AT loading in the filaments and the  
 357 sensitivity to encounter phase separation at high temperatures. Similar results were  
 358 found for a system based on hemicellulose-filled filaments (Xu et al., 2018). The  
 359 unsuccessful printing of PLA scaffold at 180°C is referred to the failure of the first layer  
 360 that should be stuck to the building platform. This might due to the fast cooling of  
 361 extruded PLA before bonding to the building platform or to the poor flowability of PLA  
 362 at 180°C. In other words, the addition of AT reduced the melting viscosity of PLA  
 363 polymer (rheology behavior data in supplementary material, Figure S1), thus improved  
 364 the printability even at low temperature.

365 *Table 5. SEM images of printed scaffolds at different 3D printing temperatures*

Temperature	180°C	200°C	220°C
PLA	Failed to print the scaffold.		



366 **4. Conclusions**

367 This study investigated the properties and 3D printability of a composite made from  
 368 PLA and acetylated tannin. The acetylation of tannin contributed to its well dispersion  
 369 within PLA matrix, guaranteeing successful fabrication of PLA/AT composite filaments  
 370 via a twin-screw extruder. PLA incorporated with 20 wt% acetylated tannin did not  
 371 significantly encounter deterioration in tensile property of the final product. Meanwhile,  
 372 the incorporation of various AT contents caused no significant effect on the melting and  
 373 glass transition temperatures of PLA because it has little influence on intermolecular  
 374 interactions or chain flexibility of PLA polymer chain. A decrease of crystallinity was  
 375 found in PLA/AT composites, resulting in higher rates of degradation in aquatic system  
 376 especially under alkaline conditions, which would definitely benefit in short-term  
 377 applications like implantable devices in biomedical field. A 3D printing temperature

378 below 250°C is suggested for safe processing of PLA/AT composites without  
379 encountering decomposition according to the data of thermogravimetric analysis.  
380 Although PLA systems loaded with acetylated tannin showed good printability in  
381 general, this is limited to temperatures reasonably below 220°C to avoid printing defects  
382 caused by phase separation and aggregation of acetylated tannin, especially at high  
383 loading content.

384

#### 385 **Author contributions**

386 The manuscript was written through contributions of all authors. All authors have  
387 given approval to the final version of the manuscript.

388

#### 389 **Conflict of interest**

390 The authors declared that they have no conflicts of interest.

#### 391 **Acknowledgement**

392 This work was supported by the National Natural Science Foundation of China  
393 (NSFC 31760187, 31971595); Natural Science Foundation of Yunnan (2017FB060); and  
394 the Yunnan provincial youth and middle-age reserve talents of academic and technical  
395 leaders (2019HB026). LERMAB is supported by the French National Research Agency  
396 through the Laboratory of Excellence ARBRE (ANR-12-LABXARBRE-01). Pascal  
397 Xanthopoulos and Polybridge® are thanked for the fruitful discussions. Financial support  
398 from China Scholarship Council is gratefully acknowledged. The authors also thank  
399 Richard Laine for precious technical support.

400

#### 401 **5. References**

402 Ambrogi, V., Cerruti, P., Carfagna, C., Malinconico, M., Marturano, V., Perrotti, M.,  
403 Persico, P., 2011. Natural antioxidants for polypropylene stabilization. *Polym.*  
404 *Degrad. Stab.* 96, 2152–2158.  
405 <https://doi.org/10.1016/j.polymdegradstab.2011.09.015>

406 Anwer, M., Naguib, H.E., Celzard, A., Fierro, V., 2015. Comparison of the thermal,  
407 dynamic mechanical and morphological properties of PLA-Lignin & PLA-Tannin  
408 particulate green composites. *Compos Part B Eng* 82, 92–99.  
409 <https://doi.org/10.1016/j.compositesb.2015.08.028>

410 Bajpai, P.K., Singh, I., Madaan, J., 2014. Development and characterization of PLA-  
411 based green composites: A review. *J. Thermoplast. Compos. Mater.* 27, 52–81.  
412 <https://doi.org/10.1177/0892705712439571>

413 Bakrani Balani, S., Chabert, F., Nassiet, V., Cantarel, A., 2019. Influence of printing  
414 parameters on the stability of deposited beads in fused filament fabrication of  
415 poly(lactic) acid. *Addit. Manuf.* 25, 112–121.  
416 <https://doi.org/10.1016/j.addma.2018.10.012>

417 Basu, A., Nazarkovsky, M., Ghadi, R., Khan, W., Domb, A.J., 2017. Poly(lactic  
418 acid)- based nanocomposites. *Polym. Adv. Technol.* 28, 919–930.  
419 <https://doi.org/10.1002/pat.3985>

420 Boruvka, M., Behalek, L., Lenfeld, P., Ngaowthong, C., Pechociakova, M., 2019.  
421 Structure-related properties of bionanocomposites based on poly(lactic acid),  
422 cellulose nanocrystals and organic impact modifier. *Mater. Technol.* 34, 143–156.  
423 <https://doi.org/10.1080/10667857.2018.1540332>

424 Bridson, J., Kaur, J., Zhang, Z., Donaldson, L., Fernyhough, A., 2015. Polymeric  
425 flavonoids processed with co-polymers as UV and thermal stabilisers for  
426 polyethylene films. *Polym Degrad Stabil* 122, 18–24.  
427 <https://doi.org/10.1016/j.polymdegradstab.2015.10.002>

428 Cruz Sanchez, F.A., Boudaoud, H., Hoppe, S., Camargo, M., 2017. Polymer recycling in  
429 an open-source additive manufacturing context: Mechanical issues. *Addit. Manuf.*  
430 17, 87–105. <https://doi.org/10.1016/j.addma.2017.05.013>

431 Dong, J., Li, M., Zhou, L., Lee, S., Mei, C., Xu, X., Wu, Q., 2017. The influence of  
432 grafted cellulose nanofibers and postextrusion annealing treatment on selected  
433 properties of poly(lactic acid) filaments for 3D printing. *J. Polym. Sci. Part B*  
434 *Polym. Phys.* 55, 847–855. <https://doi.org/10.1002/polb.24333>

435 Elsayy, M.A., Kim, K.-H., Park, J.-W., Deep, A., 2017. Hydrolytic degradation of  
436 polylactic acid (PLA) and its composites. *Renew. Sustain. Energy Rev.* 79, 1346–  
437 1352. <https://doi.org/10.1016/j.rser.2017.05.143>

438 Filgueira, D., Holmen, S., Melbø, J.K., Moldes, D., Echtermeyer, A.T., Chinga-Carrasco,  
439 G., 2017. Enzymatic-Assisted Modification of Thermomechanical Pulp Fibers To  
440 Improve the Interfacial Adhesion with Poly(lactic acid) for 3D Printing. *ACS*  
441 *Sustain. Chem. Eng.* 5, 9338–9346.  
442 <https://doi.org/10.1021/acssuschemeng.7b02351>

443 Fu, S.-Y., Feng, X.-Q., Lauke, B., Mai, Y.-W., 2008. Effects of particle size,  
444 particle/matrix interface adhesion and particle loading on mechanical properties  
445 of particulate–polymer composites. *Compos. Part B Eng.* 39, 933–961.  
446 <https://doi.org/10.1016/j.compositesb.2008.01.002>

447 García, D., Glasser, W., Pizzi, A., Paczkowski, S., Laborie, M.-P., 2015. Modification of  
448 condensed tannins: from polyphenol chemistry to materials engineering. *New J*  
449 *Chem* 40, 36–49. <https://doi.org/10.1039/C5NJ02131F>

450 García, D.E., Glasser, W.G., Pizzi, A., Paczkowski, S., Laborie, M.-P., 2015.  
451 Hydroxypropyl tannin from *Pinus pinaster* bark as polyol source in urethane

452 chemistry. Eur. Polym. J. 67, 152–165.  
 453 <https://doi.org/10.1016/j.eurpolymj.2015.03.039>  
 454 Gaugler, M., Grigsby, W., Harper, D., Rials, T., 2007. Chemical imaging of the spatial  
 455 distribution and interactions of tannin dispersal in bioplastic systems. *Adv. Mater.*  
 456 *Res.* 29–30, 173–176. <https://doi.org/10.4028/www.scientific.net/AMR.29-30.173>  
 457 Ge, J., Shi, X., Cai, M., Wu, R., Wang, M., 2003. A novel biodegradable antimicrobial  
 458 PU foam from wattle tannin. *J. Appl. Polym. Sci.* 90, 2756–2763.  
 459 <https://doi.org/10.1002/app.12928>  
 460 Gkartzou, E., Koumoulos, E.P., Charitidis, C.A., 2017. Production and 3D printing  
 461 processing of bio-based thermoplastic filament. *Manuf. Rev.* 4, 1.  
 462 <https://doi.org/10.1051/mfreview/2016020>  
 463 Grigsby, W., Bridson, J., Lomas, C., Frey, H., 2014. Evaluating Modified Tannin Esters  
 464 as Functional Additives in Polypropylene and Biodegradable Aliphatic Polyester.  
 465 *Macromol Mater Eng* 299, 1251–1258. <https://doi.org/10.1002/mame.201400051>  
 466 Grigsby, W., Kadla, J., 2014. Evaluating Poly(lactic acid) Fiber Reinforcement with  
 467 Modified Tannins. *Macromol Mater Eng* 299, 368–378.  
 468 <https://doi.org/10.1002/mame.201300174>  
 469 Grigsby, W.J., Bridson, J.H., Lomas, C., Elliot, J.-A., 2013. Esterification of Condensed  
 470 Tannins and Their Impact on the Properties of Poly(Lactic Acid). *Polymers* 5,  
 471 344–360. <https://doi.org/10.3390/polym5020344>  
 472 Grigsby, W.J., Bridson, J.H., Schrade, C., 2015. Modifying biodegradable plastics with  
 473 additives based on condensed tannin esters. *J Appl Polym Sci* 132, 41626.  
 474 <https://doi.org/10.1002/app.41626>  
 475 Guo, R., Ren, Z., Bi, H., Song, Y., Xu, M., 2018. Effect of toughening agents on the  
 476 properties of poplar wood flour/poly (lactic acid) composites fabricated with  
 477 Fused Deposition Modeling. *Eur. Polym. J.* 107, 34–45.  
 478 <https://doi.org/10.1016/j.eurpolymj.2018.07.035>  
 479 Hussain, T., Tausif, M., Ashraf, M., 2015. A review of progress in the dyeing of eco-  
 480 friendly aliphatic polyester-based polylactic acid fabrics. *J. Clean. Prod.* 108,  
 481 476–483. <https://doi.org/10.1016/j.jclepro.2015.05.126>  
 482 Kai, D., Tan, M.J., Chee, P.L., Chua, Y.K., Yap, Y.L., Loh, X.J., 2016. Towards lignin-  
 483 based functional materials in a sustainable world. *Green Chem.* 18, 1175–1200.  
 484 <https://doi.org/10.1039/C5GC02616D>  
 485 Karamanlioglu, M., Preziosi, R., Robson, G.D., 2017. Abiotic and biotic environmental  
 486 degradation of the bioplastic polymer poly(lactic acid): A review. *Polym. Degrad.*  
 487 *Stab.* 137, 122–130. <https://doi.org/10.1016/j.polymdegradstab.2017.01.009>  
 488 Koleckar, V., Kubikova, K., Rehakova, Z., Kuca, K., Jun, D., Jahodar, L., Opletal, L.,  
 489 2008. Condensed and hydrolysable tannins as antioxidants influencing the health.  
 490 *Mini Rev. Med. Chem.* 8, 436–447. <https://doi.org/10.2174/138955708784223486>  
 491 Lai So, V.L., He, L., Xin, J.H., 2014. Bio-inspired colouration on various textile  
 492 materials using a novel catechol colorant. *RSC Adv* 4, 41081–41086.  
 493 <https://doi.org/10.1039/C4RA06004K>  
 494 Lee, J.-Y., An, J., Chua, C.K., 2017. Fundamentals and applications of 3D printing for  
 495 novel materials. *Appl. Mater. Today* 7, 120–133.  
 496 <https://doi.org/10.1016/j.apmt.2017.02.004>  
 497 LI, T., Aspler, J., Kingsland, A., 2016. 3D PRINTING – A REVIEW OF

498 TECHNOLOGIES, MARKETS, AND OPPORTUNITIES FOR THE FOREST  
 499 INDUSTRY. *Can. Makes*. URL [http://canadamakes.ca/3d-printing-review-](http://canadamakes.ca/3d-printing-review-technologies-markets-opportunities-forest-industry/)  
 500 [technologies-markets-opportunities-forest-industry/](http://canadamakes.ca/3d-printing-review-technologies-markets-opportunities-forest-industry/) (accessed 12.4.19).

501 Liao, J., Brosse, N., Pizzi, A., Hoppe, S., 2019. Dynamically Cross-Linked Tannin as a  
 502 Reinforcement of Polypropylene and UV Protection Properties. *Polymers* 11, 102.  
 503 <https://doi.org/10.3390/polym11010102>

504 Liu, J., Sun, L., Xu, W., Wang, Q., Yu, S., Sun, J., 2019. Current advances and future  
 505 perspectives of 3D printing natural-derived biopolymers. *Carbohydr. Polym.* 207,  
 506 297–316. <https://doi.org/10.1016/j.carbpol.2018.11.077>

507 Long, H., Wu, Z., Dong, Q., Shen, Y., Zhou, W., Luo, Y., Zhang, C., Dong, X., 2019.  
 508 Mechanical and thermal properties of bamboo fiber reinforced  
 509 polypropylene/polylactic acid composites for 3D printing. *Polym. Eng. Sci.* 59,  
 510 E247–E260. <https://doi.org/10.1002/pen.25043>

511 Luo, C., Grigsby, W., Edmonds, N., Eastal, A., Al-Hakkak, J., 2010. Synthesis,  
 512 characterization, and thermal behaviors of tannin steirates prepared from  
 513 quebracho and pine bark extracts. *J. Appl. Polym. Sci.* 17, 352–360.  
 514 <https://doi.org/10.1002/app.31545>

515 Lyu, S., Untereker, D., 2009. Degradability of Polymers for Implantable Biomedical  
 516 Devices. *Int. J. Mol. Sci.* 10, 4033–4065. <https://doi.org/10.3390/ijms10094033>

517 Müller, A.J., Ávila, M., Saenz, G., Salazar, J., 2014. CHAPTER 3. Crystallization of  
 518 PLA-based Materials, in: Jiménez, A., Peltzer, M., Ruseckaite, R. (Eds.), *Polymer*  
 519 *Chemistry Series*. Royal Society of Chemistry, Cambridge, pp. 66–98.  
 520 <https://doi.org/10.1039/9781782624806-00066>

521 Murariu, M., Dubois, P., 2016. PLA composites: From production to properties. *Adv.*  
 522 *Drug Deliv. Rev.*, PLA biodegradable polymers 107, 17–46.  
 523 <https://doi.org/10.1016/j.addr.2016.04.003>

524 Nguyen, N.A., Barnes, S.H., Bowland, C.C., Meek, K.M., Littrell, K.C., Keum, J.K.,  
 525 Naskar, A.K., 2018. A path for lignin valorization via additive manufacturing of  
 526 high-performance sustainable composites with enhanced 3D printability. *Sci. Adv.*  
 527 4, eaat4967. <https://doi.org/10.1126/sciadv.aat4967>

528 Nicollin, A., Zhou, X., Pizzi, A., Grigsby, W., Rode, K., Delmotte, L., 2013. MALDI-  
 529 TOF and <sup>13</sup>C NMR analysis of a renewable resource additive—Thermoplastic  
 530 acetylated tannins. *Ind. Crops Prod.* 49, 851–857.  
 531 <https://doi.org/10.1016/j.indcrop.2013.06.013>

532 Olejar, K.J., Ray, S., Kilmartin, P.A., 2016. Enhanced antioxidant activity of polyolefin  
 533 films integrated with grape tannins: Enhanced antioxidant activity of polyolefin  
 534 films integrated with grape tannins. *J. Sci. Food Agric.* 96, 2825–2831.  
 535 <https://doi.org/10.1002/jsfa.7450>

536 Pizzi, A., 1980. Tannin-Based Adhesives. *J. Macromol. Sci. Part C* 18, 247–315.  
 537 <https://doi.org/10.1080/00222358008081043>

538 Ren, J., 2011. *Biodegradable poly (lactic acid) synthesis, modification, processing and*  
 539 *applications*. Tsinghua University Press : Springer, Beijing; Heidelberg.

540 Samper, M.D., Fages, E., Fenollar, O., Boronat, T., Balart, R., 2013. The potential of  
 541 flavonoids as natural antioxidants and UV light stabilizers for polypropylene. *J.*  
 542 *Appl. Polym. Sci.* 129, 1707–1716. <https://doi.org/10.1002/app.38871>

543 Scheyer, L.E., Chiweshe, A., 2001. Application and Performance of Disperse Dyes on

544 Poly(lactic acid) (PLA) Fabric. *AATCC Mag.* 1, 44–48.

545 Shnawa, H., Khaleel, M., Muhamed, F., 2015. Oxidation of HDPE in the Presence of  
546 PVC Grafted with Natural Polyphenols (Tannins) as Antioxidant. *J. Polym. Chem.*  
547 05, 9–16. <https://doi.org/10.4236/ojpcem.2015.52002>

548 Smith, B.C., 2018. The C=O Bond, Part IV: Acid Anhydrides [WWW Document]. URL  
549 <http://www.spectroscopyonline.com/co-bond-part-iv-acid-anhydrides> (accessed  
550 4.16.19).

551 Tappa, K., Jammalamadaka, U., 2018. Novel Biomaterials Used in Medical 3D Printing  
552 Techniques. *J. Funct. Biomater.* 9. <https://doi.org/10.3390/jfb9010017>

553 Tokiwa, Y., Calabia, B.P., 2006. Biodegradability and biodegradation of poly(lactide).  
554 *Appl. Microbiol. Biotechnol.* 72, 244–251. [https://doi.org/10.1007/s00253-006-](https://doi.org/10.1007/s00253-006-0488-1)  
555 0488-1

556 Tomak, E.D., Arican, F., Gonultas, O., Sam, E.D., 2018. Influence of tannin containing  
557 coatings on weathering resistance of wood: Water based transparent and opaque  
558 coatings. <https://doi.org/10.1016/j.polymdegradstab.2018.03.011>

559 Vila, C., Santos, V., Saake, B., Parajó, J.C., 2016. Manufacture, Characterization, and  
560 Properties of Poly-(lactic acid) and its Blends with Esterified Pine Lignin.  
561 *BioResources* 11, 5322–5332. <https://doi.org/10.15376/biores.11.2.5322-5332>

562 Xu, W., Pranovich, A., Uppstu, P., Wang, X., Kronlund, D., Hemming, J., Öblom, H.,  
563 Moritz, N., Preis, M., Sandler, N., Willför, S., Xu, C., 2018. Novel biorenewable  
564 composite of wood polysaccharide and polylactic acid for three dimensional  
565 printing. *Carbohydr. Polym.* 187, 51–58.  
566 <https://doi.org/10.1016/j.carbpol.2018.01.069>

567 Yamoum, C., Maia, J., Magaraphan, R., 2017. Rheological and thermal behavior of PLA  
568 modified by chemical crosslinking in the presence of ethoxylated bisphenol A  
569 dimethacrylates 28, 102–112. <https://doi.org/10.1002/pat.3864>

570 Yew, G.H., Mohd Yusof, A.M., Mohd Ishak, Z.A., Ishiaku, U.S., 2005. Water absorption  
571 and enzymatic degradation of poly(lactic acid)/rice starch composites. *Polym.*  
572 *Degrad. Stab.* 90, 488–500.  
573 <https://doi.org/10.1016/j.polymdegradstab.2005.04.006>

574 Zhai, Y., Wang, J., Wang, H., Song, T., Hu, W., Li, S., 2018. Preparation and  
575 Characterization of Antioxidative and UV-Protective Larch Bark Tannin/PVA  
576 Composite Membranes. *Molecules* 23, 2073.  
577 <https://doi.org/10.3390/molecules23082073>

578 Zhang, L., Lv, S., Sun, C., Wan, L., Tan, H., Zhang, Y., 2017. Effect of MAH-g-PLA on  
579 the Properties of Wood Fiber/Poly(lactic acid) Composites. *Polymers* 9, 591.  
580 <https://doi.org/10.3390/polym9110591>

581

582